



ELSEVIER

Contents lists available at ScienceDirect

## Deep-Sea Research I

journal homepage: [www.elsevier.com/locate/dsrI](http://www.elsevier.com/locate/dsrI)

## Instruments and Methods

## An evaluation of deep-sea benthic megafauna length measurements obtained with laser and stereo camera methods

Katherine M. Dunlop<sup>a,\*</sup>, Linda A. Kuhnz<sup>a</sup>, Henry A. Ruhl<sup>b</sup>, Christine L. Huffard<sup>a</sup>, David W. Caress<sup>a</sup>, Richard G. Henthorn<sup>a</sup>, Brett W. Hobson<sup>a</sup>, Paul McGill<sup>a</sup>, Kenneth L. Smith Jr<sup>a</sup><sup>a</sup> Monterey Bay Aquarium Research Institute, 7700 Sandholdt Road, Moss Landing, CA 93940, USA<sup>b</sup> National Oceanography Centre, European Way, Southampton SO14 3ZH, UK

## ARTICLE INFO

## Article history:

Received 11 August 2014

Received in revised form

5 November 2014

Accepted 11 November 2014

Available online 28 November 2014

## Keywords:

Deep-sea megafauna

Benthic communities

Stereo camera

Biomass

## ABSTRACT

The 25 year time-series collected at Station M, ~4000 m on the Monterey Deep-sea Fan, has substantially improved understanding of the role of the deep-ocean benthic environment in the global carbon cycle. However, the role of deep-ocean benthic megafauna in carbon bioturbation, remineralization and sequestration is relatively unknown. It is important to gather both accurate and precise measurements of megafaunal community abundance, size distribution and biomass to further define their role in deep-sea carbon cycling and possible sequestration. This study describes initial results from a stereo camera system attached to a remotely operated vehicle and analyzed using the EventMeasure photogrammetric measurement software to estimate the density, length and biomass of 10 species of mobile epibenthic megafauna. Stereo length estimates were compared to those from a single video camera system equipped with sizing lasers and analyzed using the Monterey Bay Aquarium Research Institute's Video Annotation and Reference System. Both camera systems and software were capable of high measurement accuracy and precision ( $< \pm 1$  mm measurement error and precision). However, the oblique angle of the single video camera caused the spatial scale of the image perspective to change with distance from the camera, resulting in error when measurements were not parallel or vertical to two horizontal-oriented scaling lasers. Analysis showed that the stereo system recorded longer lengths and higher biomass estimates than the single video camera system for the majority of the 10 megafauna species studied. The stereo image analysis process took substantially longer than the video analysis and the value of the EventMeasure software tool would be improved with developments in analysis automation. The stereo system is less influenced by object orientation and height, and is potentially a useful tool to be mounted on an autonomous underwater vehicle and for measuring deep-sea pelagic animals where the use of lasers is not feasible.

© 2014 The Authors. Published by Elsevier Ltd. This is an open access article under the CC BY-NC-ND license (<http://creativecommons.org/licenses/by-nc-nd/4.0/>).

## 1. Introduction

Data continue to be collected at Station M, ~4000 m at the Monterey Deep-sea Fan, adding to a 25 year time-series that has substantially improved understanding of the connections between surface food supply and deep-ocean benthic communities and the role of the deep-ocean benthic environment in the global carbon cycle (Smith et al., 2014). The role of carbon bioturbation, remineralization and sequestration by deep-ocean benthos in the global carbon cycle is, however, relatively unknown and potentially highly variable over time (Smith et al., 2013, 2014). Deep-sea epibenthic megafauna are animals (usually  $\geq 1$  cm) that occupy the surface layer of seabed sediment and are visible in

photographs (Grassle et al., 1975; Smith et al., 1993). This group makes a significant contribution to the deep-sea benthic biomass (Haedrich and Rowe, 1977; Lauerman et al., 1996) and represents the dominant animals observed in time-lapse photographs of the seafloor taken at Station M. Epibenthic megafauna play a role in deep-sea carbon sequestration through the redistribution of organic material, oxygen and nutrients in the sediment surface layers, and remineralization of organic carbon (Smith et al., 1993). Megafauna community composition, abundance and size distribution vary in response to climate-induced changes, in particulate organic carbon supply to the seafloor (Ruhl and Smith, 2004), and have been suggested as an indicator group in terms of understanding the effects of climatic variation on abyssal benthos (Ruhl, 2007).

It is important to improve our knowledge of the abundance, size distribution, biomass, spatial distribution and movement patterns of megafaunal animals in order to further define their

\* Corresponding author.

E-mail address: [kdunlop@mbari.org](mailto:kdunlop@mbari.org) (K.M. Dunlop).

role in the deep-sea carbon cycle. This information will also lead to a better understanding of community responses to changes in food supply and demographic variation, as well as their impact on biogeochemical cycling (Lauerman et al., 1996). Biomass estimates are required to calculate the organic carbon utilization of epibenthic megafauna using wet-weight specific oxygen consumption rates of individual species (Ruhl et al., 2013). Significant advances in our understanding of the role of deep-sea benthic communities in the global carbon cycle are expected to result from combining estimates of organic carbon utilization of the epibenthic megafaunal community with time-series data on surface food supply, sediment community oxygen consumption (a measure of the total benthic community oxygen utilization, and a proxy for carbon consumption) and community composition collected at Station M.

Body size measurements of animals that are both accurate (i.e. close to the true size), and precise (repeatable), with low variability around the mean, are necessary for reliable biomass estimates (Abdo et al., 2006; Harvey and Shortis, 1998). Estimates of deep-sea benthic megafauna density and body size have been made using trawls and dredges (Lampitt et al., 1986). These extractive methods allow for high quality data on size-mass relationships and taxonomy of megafauna species (Christiansen and Thiel, 1992). These data have been combined with photogrammetric techniques to collect quantitative data on community abundance and distribution (Lauerman et al., 1996; Ruhl, 2007). Between 1989 and 2004 mobile megafaunal organism density and body size data were estimated at Station M using towed camera surveys (Ruhl, 2007). Oblique photographs from a towed camera were projected onto a perspective grid and digitized to quantify the area in each photograph (Wakefield and Genin, 1987; Ruhl, 2007; Lauerman et al., 1996; Kaufmann and Smith, 1997). The position and size of animals was measured in relation to the grid with an accuracy of between 3 and 5 mm (Lauerman et al., 1996; Kaufmann and Smith, 1997; Lauerman and Kaufmann, 1998). The body size data generated by this method were analyzed in relation to abundance trends for dominant megafaunal species to estimate individual species growth rates (Ruhl, 2007). Since 2006, megafauna body size at Station M has been measured from video recorded by a camera mounted on remotely operated vehicles (ROVs) (Kuhnz et al., 2014). This method involves the use of paired lasers to provide a scale bar on the seafloor against which length measurements can be calibrated in frame grabs (Kuhnz et al., 2014). Paired lasers are commonly used to provide a scale in ROV recordings (Barker et al., 2001; Rochet et al., 2006) but require that the camera is orientated along an axis parallel or perpendicular to the lasers for maximum accuracy (Rochet et al., 2006). The incorporation of additional lasers for a four-laser system has enabled both the distance and orientation of the target plane in relation to the camera to be determined. This system enables scale to be provided to oblique angle target planes using two algorithms implemented in the software Laser Measure<sup>®</sup> (Barker et al., 2001). ROVs provide a stable platform on which the cameras can be accurately positioned to make measurements using the lasers (Barker et al., 2001). An oblique view of the seafloor is commonly employed with ROVs, facilitating operation of the vehicle and providing appropriate lighting for species identification and habitat features. The Monterey Bay Aquarium Research Institute's (MBARI) Video Annotation and Reference System (VARS) was developed to annotate, categorize, store, and retrieve information about objects and events of interest from video and images collected from static observation platforms and ROVs (Schlinding and Stout, 2006). This software was used to record annotations of epibenthic megafauna density from ROV transects at Station M (Kuhnz et al., 2014).

Stereo photogrammetry has been used to gather size measurements of shallow marine epibenthic organisms including sponges (Abdo et al., 2006) and hard corals (Done, 1982), but primarily to estimate the diversity, relative abundance and size structure of

both demersal (Moore et al., 2010) and pelagic marine fishes (Santana-Garcon et al., 2014). Stereo photogrammetry techniques have been introduced to deep-sea baited landers to investigate, for example, the scavenger communities of the deep Arabian Sea between 3190 and 4420 m (Janßen et al., 2000) and the relative abundance and size of Gulper sharks (*Centrophorus* sp) on the upper slope (up to 1000 m depth) of the continental shelf of Eastern Australia (Marouchos et al., 2011). A towed stereo video system has also been designed to survey deep marine benthic habitats (up to 1200 m depth) during the design of offshore marine protected areas in South Eastern Australia (Shortis et al., 2007). Harvey and Shortis (1998) hypothesized that changes in the refractive index of the water due to changes in pressure, temperature and salinity at depth might lead to inaccuracies when stereo measurements, based on shallow-water calibration parameters, were made during these deeper deployments. Measurements from a towed stereo-video system up to 2000 m depth had a maximum measurement error of 8% (Shortis et al., 2007).

The objectives of this current study were to compare (1) the effect of depth (~4000 m) on length measurements made by a stereo still camera system calibrated in shallow water, (2) the accuracy and precision of measurements of calibration targets by a stereo still and a single underwater video camera system (hereafter called the mono video camera system) and software and (3) the length estimates of 10 common mobile epibenthic megafauna species recorded by these two photographic methods simultaneously at Station M. Results are interpreted to provide guidelines to maximize the accuracy and precision of epibenthic megafauna body size measurements and biomass estimates collected using these two camera methods at Station M.

## 2. Material and methods

### 2.1. Stereo still camera equipment

The stereo camera system used here consists of two high-resolution digital color still cameras (Prosilica GX1920, 2.4 Mpixel) configured as a stereo pair. The cameras have a 5 mm wide-angle lens and corrective optics for operation in water. Each camera is secured in a dome port titanium housing and held rigidly in place in the internal case with a cantilever bracket. The cameras are mounted in parallel on a metal base bar facing vertically downwards toward the seafloor. During this study the cameras were separated by either 200 or 600 mm on the base bar to examine the effect of camera separation on measurement accuracy and precision. The relative orientation of the cameras is maintained with a stabilizing bracket around the two external housings. Two Ocean Imaging Systems 3831 strobes (200W-s total) are mounted on either side of the cameras and also angled vertically. Two housings containing the power electronics, the strobe and camera control electronics, and the network link to the ROV tether are mounted behind the cameras (Fig. 1). The whole unit is mounted on a drawer placed on the underside of the ROV *Doc Ricketts* and is designed to be routinely deployed to 4000 m depth. Linux-based camera software synchronizes the capture of paired images and achieves real time transfer of the digital images to a shipboard laptop computer.

### 2.2. Stereo camera system calibration

Cameras were calibrated in less than 1 m depth in the MBARI test tank before and after data collection, using the techniques developed by Shortis and Harvey (1998). The calibration uses multiple images of a three-dimensional aluminum control cuboid frame with dimensions of 1 × 1 × 0.5 m and marked with 80

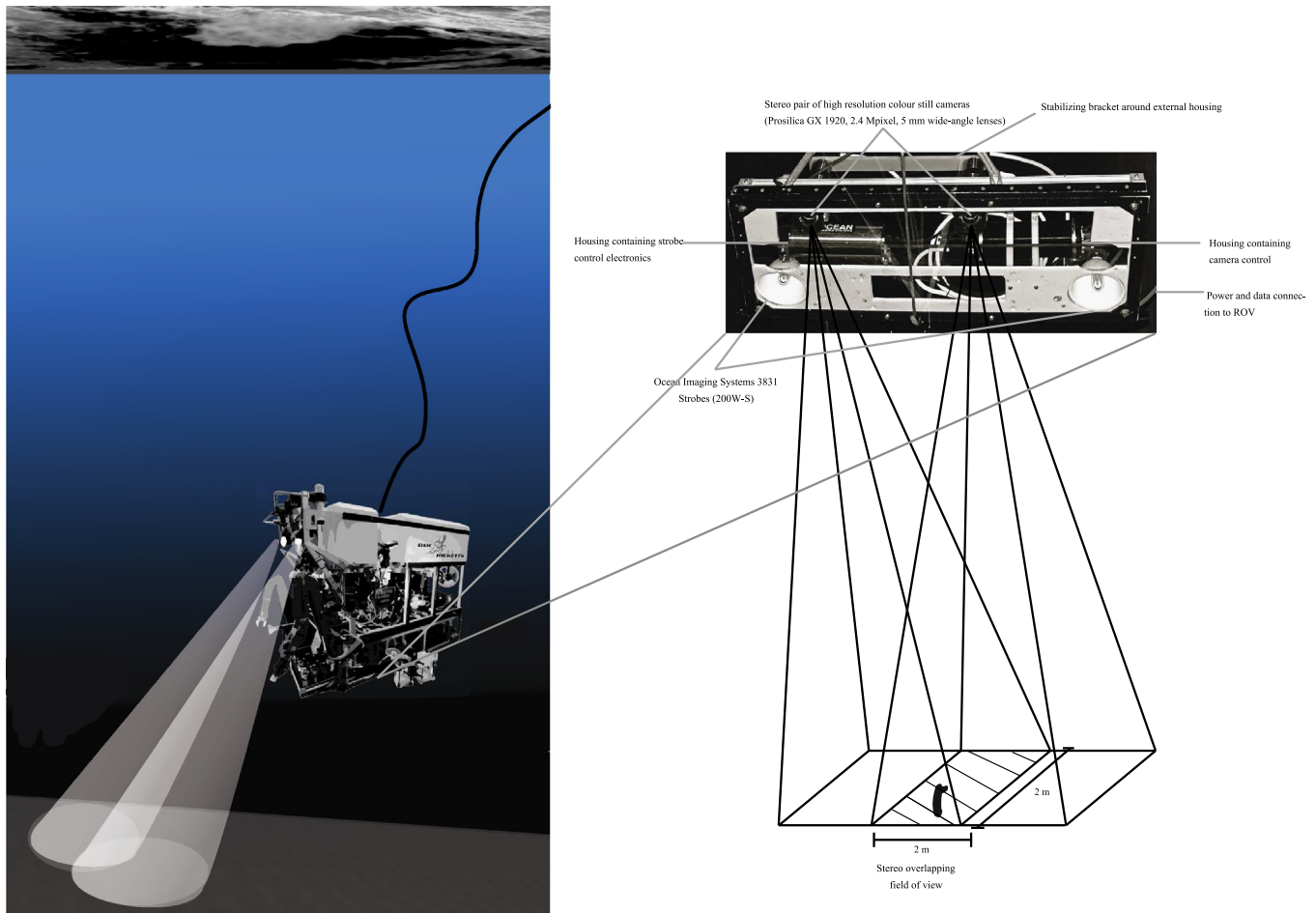


**Fig. 1.** Diagram illustrating the stereo underwater camera equipment measuring an individual *Psychropotes longicauda*. The stereo camera is mounted on the underside on the remotely operated vehicle *Doc Ricketts*.

precisely known reference points. This will be referred to as the calibration cube. The locations of these points were measured in multiple images taken from 20 positions relative to the control frame. The images are analyzed in SeaGIS CAL software (<http://www.seagis.com.au>) using a self-calibrating photogrammetric network solution to calibrate both the internal and external parameters of the camera. Calibration files were created for both cameras accounting for the vertical and horizontal alignment of the camera, their relative orientation and the cameras' optical properties. The cameras were calibrated in two orientations: one with 200 mm separation between the cameras and another with 600 mm separation.

### 2.3. Mono video camera equipment

The mono video camera system is a high-definition Ikegama video camera fitted with HA10Xt.2 Fujinon lens with two LED lights (Deepsea Power and Light, Matrix-3 SeaLite) mounted on the front of the ROV *Doc Ricketts* facing at a forward-oblique angle, between 40 and 45°, towards the seabed. The video camera was set at an oblique angle to facilitate species identification. The red lasers with parallel beams, which provided high-contrast colour against the seafloor (Power Technology Inc., PM12 635-15C), were mounted 29 cm apart. The distance between the laser dots, as well as their size, thus varies with the altitude of the ROV above the seafloor, and act as a reference for measurements and to help maintain a consistent 1 m transect width at an altitude between 2 and 3 m.

### 2.4. Mono video camera system calibration

The lasers were calibrated to verify the 29 cm distance apart on deck prior to the ROV deployment. This was achieved by placing a calibration checkerboard with squares measuring 29 cm in front of the mono video camera.

### 2.5. Surveys

Surveys were recorded at Station M (35°10'N, 122°59'W), about 4000 m water depth in an abyssal region of the Northeast Pacific, ca. 200 km off the Central California coast, where deep-ocean processes have been studied in relation to atmospheric and surface ocean conditions since 1989 (Smith et al., 2013). The seafloor at Station M consists of silty-clay sediments and minimal bathymetric relief (Kaufmann and Smith, 1997). Primary productivity at Station M is highly seasonal and closely linked to upwelling events in the California Current (Pelaez and McGowan, 1986) leading to clear seasonal patterns in the flux of particulate organic matter to the seafloor (Smith et al., 1992) and changes in the benthic community (Ruhl, 2008; Kuhnz et al., 2014).

The ROV was deployed from the R/V *Western Flyer*. Stereo images and ROV video footage were recorded simultaneously for two 1 km transects. Transect one was recorded on the 16th June 2013 with the stereo camera system in orientation one (200 mm separation between the cameras) and transect two on the 4th April 2014 in stereo camera orientation two (600 mm separation between the cameras). The ROV flew at an altitude of ~2 m above

bottom, allowing for a stereo field of view  $\sim 4 \text{ m}^2$  and a video field of view of  $1 \text{ m}^2$ . However, only the overlapping  $1 \text{ m}$  by  $1 \text{ m}$  transect length observed by both camera systems was analyzed. Video footage was recorded continuously, while stereo pairs of still color images were taken every 2 s.

Stereo images of a second, smaller calibration cube ( $0.5 \times 0.5 \times 0.3 \text{ m}$ ) taken from a distance of  $1 \text{ m}$  in the test tank,  $< 1 \text{ m}$  below the surface, were used to assess the effects of water depth on stereo measurements. Four lengths between reference points on the calibration cube and checkerboard were measured ten times in stereo images and VARS footage to compare the length measurement accuracy and precision. Checkerboard lengths ranged between  $20$  to  $325 \text{ mm}$  and were at vertical, horizontal and diagonal orientations in relation to the VARS lasers to examine the effect of size and orientation on the measurement accuracy and precision.

## 2.6. Image analysis and data collection

Approximately 5000 stereo images were collected in both transects one and two. Some overlapping stereo images were removed to provide a continuous  $1 \text{ km}$  long section of seabed imagery. Images and videos were annotated for the presence of the 10 dominant mobile megafauna species (*Elpidia* sp. A, *Oneirophanta mutabilis* complex, *Peniagone gracilis*, *Peniagone papillata*, *Peniagone* sp. 1, *Peniagone* sp. 2, *Peniagone* sp. A, *Peniagone vitrea*, *Psychropotes longicauda* and *Scotoplanes globosa*). These species represent a significant proportion of the megafauna observed at Station M (Kuhnz et al., 2014) and length/biomass relationships have been described for these, or closely related, species (Ruhl et al., 2013). To estimate these relationships, length measurements of fresh specimens were made at the longest dimension from the anterior to posterior, excluding the appendages, as described by Ruhl (2007).

The program EventMeasure (SeaGIS Pty Ltd, Bacchas Marsh, Victoria, Australia) was used to measure the length of megafauna from stereo images. The software simultaneously calculates the distance of the camera to the seabed and the length of objects in the field of view using the photogrammetric network computed during the calibration (Langlois et al., 2012). The method has enabled accurate and precise length and biomass estimates of fish from baited remote underwater stereo video systems in shallow water (Harvey et al., 2012). For measurements, stereo-pairs of images were matched and the same front and end points of each individual within each image were manually selected (Fig. 2). The coordinates of the paired points were converted into three-dimensional object space ( $x$ ,  $y$  and  $z$ ) (Harvey et al., 2002a). The distance and angle of the points in relation to the central point of the camera lenses were also calculated (Harvey and Shortis, 1995).

To make a measurement using VARS, a frame grab from the video from the mono video camera system was taken whereby the center of each object or organism was aligned, at the same level, with the paired lasers in the video footage. This criterion for video selection aimed to minimize measurement distortion. Targets (a calibration cube, and a flat checkerboard) or animals, were measured in different orientations, such as vertical, horizontal or diagonal, to the lasers (Fig. 3). The top of the calibration cube sat  $30 \text{ cm}$  above the seafloor and was used to detect errors in measurements of objects above the seafloor.

Next, measurements were taken of the reference distance between the lasers and then the calibration target or organism using the VARS distance tool. The distance tool converts the measurement of the organism from pixel length to a length measurement using an algorithm based on the known distance between the lasers. The time taken to organize, identify, and measure the 10 megafauna species from the stereo images and video footage was recorded. Megafauna length estimates from both the stereo and mono video camera were converted to biomass using conversion equations calculated from length-weight relationships of the species, or closely related species (Ruhl et al., 2013).

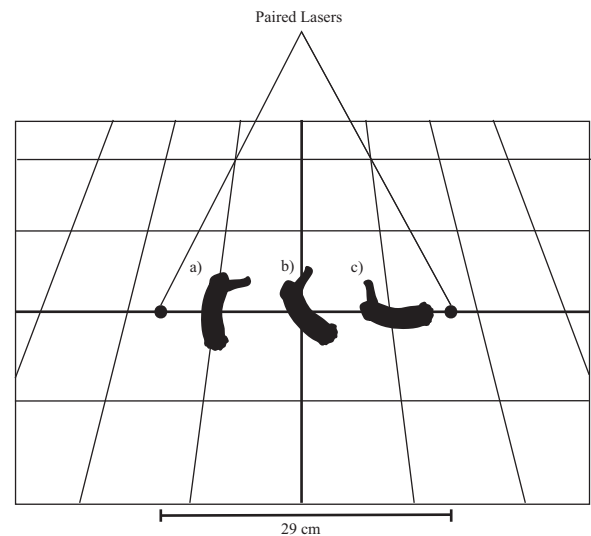


Fig. 3. Diagram illustrating an individual *Psychropotes longicauda* aligned with the paired lasers in (a) vertical, (b) diagonal and (c) horizontal orientations in the Video Annotation and Reference System. The diagram is projected onto the Canadian perspective grid.

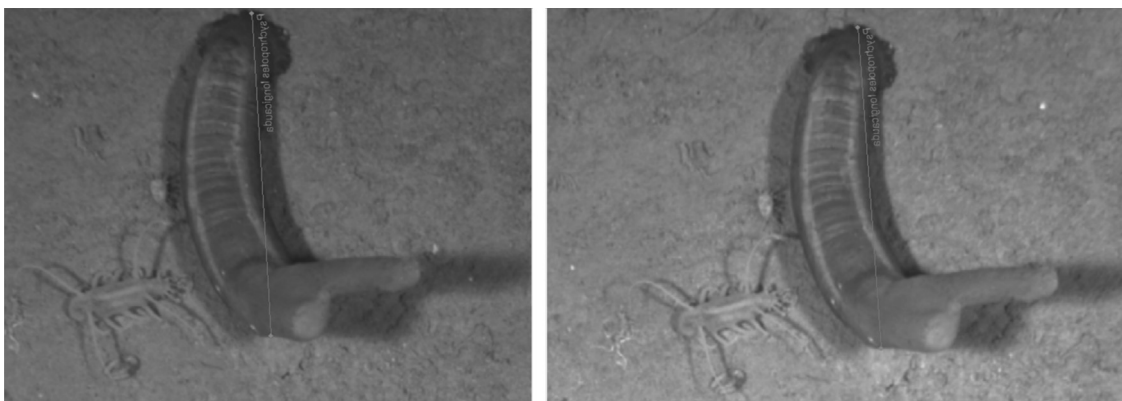


Fig. 2. Stereo pair of images of *Psychropotes longicauda* from the stereo measurement software EventMeasure.

## 2.7. Data analysis

The accuracy of stereo measurements was calculated as the mean error ( $\pm$  mm) between each length estimate ( $\hat{V}$ ) and the true length ( $V$ ) as measured by an engineering ruler. Values greater than one indicated that measurements were overestimated and less than one represented that measurements were underestimated. Precision was measured as the variability around the mean and was calculated as the standard deviation. A lower standard deviation indicates an improved precision. Calibration target measurement accuracy and precision data were tested using a Shapiro–Wilks normality test and a Levene's test for equal variance and compared between depths and camera methods using the nonparametric Kruskal–Wallis rank sum test for groups and Wilcoxon rank sum test for pairwise comparisons in the statistical package R (version 3.0.2, The R Development Core Team, 2011). Megafaunal density, length and biomass estimates recorded by the stereo and mono camera methods were compared using a nonparametric Mann–Whitney  $U$  test (Conover, 1980) in R.

## 3. Results

### 3.1. The effect of depth on stereo still camera length measurements

No significant difference was found between the stereo length measurements of the small calibration cube in the test tank and at depth ( $H=0.06$ ,  $N=40$ ,  $p > 0.05$ ).

### 3.2. The accuracy and precision of measurements of calibration targets by stereo still and mono video cameras

The mean accuracy of mono video camera measurements of flat checkerboard lengths both horizontally and vertically orientated to the lasers were  $< 1$  mm and were not significantly different from stereo length measurements ( $H=0.54$ ,  $N=40$ ,  $p > 0.05$ ). VARS measurements that were at a diagonal orientation to the lasers were significantly underestimated ( $H=14.30$ ,  $N=40$ ,  $p < 0.001$ ) compared to the stereo system measurements (Table 1a and b; Fig. 4a). The precision of VARS checkerboard measurements were not statistically different ( $H=0.33$ ,  $N=40$ ,  $p > 0.05$ ) from stereo measurements (Table 1a and b; Fig. 4b).

The mean accuracy of all mono video camera length measurements of the 30-cm tall calibration cube was significantly lower ( $H=5.14$ ,  $N=40$ ,  $p < 0.05$ ) than the accuracy of stereo camera measurements. The accuracy of mono video camera measurements was highest when both lasers were on the cube and lowest when both lasers were on the seabed. Stereo measurements of the cube made at the edge of the image had a significantly higher mean accuracy ( $H=12.74$ ,  $N=40$ ,  $p < 0.005$ ) than measurements in the middle when the cameras were separated by 200 mm. When the stereo camera separation was increased to 600 mm, the mean accuracy of edge measurements significantly decreased ( $H=16.41$ ,  $N=40$ ,  $p < 0.05$ ) but a significant difference ( $H=24.49$ ,  $N=40$ ,  $p < 0.005$ ) between the middle and edge measurements was still detected (Table 1a and b; Fig. 5a). However, this difference is small enough to have little biological relevance. The mean precision of cube measurements was not significantly different ( $H=2.01$ ,  $N=20$ ,  $p > 0.05$ ) between mono and stereo measurements. The mean precision of stereo measurements made at the image edges was significantly ( $H=8.65$ ,  $N=40$ ,  $p < 0.001$ ) poorer than those made in the middle. Edge precision significantly improved ( $H=6.70$ ,  $N=40$ ,  $p < 0.01$ ) with the separation of the cameras to 600 mm (Table 1a and b; Fig. 5b).

### 3.3. Epibenthic megafauna density, length and biomass estimates

All 10 targeted megafauna species were present in both transects except *P. sp. 1*, which was absent in transect two. In transect one *P. sp. A*, *E. sp. A* and *S. globosa* were the highest density species and in transect two, the density estimates of *E. sp. A* had declined, leaving *P. sp. A* and *S. globosa* to dominate. There was no significant difference in either transect one ( $V=22$ ,  $N=10$ ,  $p > 0.05$ ) or two ( $V=8$ ,  $N=10$ ,  $p > 0.05$ ) in the density (individuals  $m^{-2}$ ) of any species recorded by the mono video camera/VARS and the stereo camera/EventMeasure methods (Figs. 6a and 7a).

Stereo length measurements of *E. sp. A*, *P. gracilis*, *P. papillata*, *P. sp. 1*, *P. sp. A*, *P. vitrea*, and *S. globosa* in transect one were significantly longer (all  $p < 0.001$ ) than mono measurements (Fig. 6b). In transect two the stereo length measurements of *E. sp. A*, *P. gracilis*, *P. sp. A*, *P. vitrea*, *S. globosa* and *P. papillata* were also significantly longer (all  $p < 0.05$ ) than mono video camera measurements (Fig. 7b).

The total estimated biomass of the 10 species recorded in transect one by the stereo camera system was 24.96 kg, which was

**Table 1**  
Mean error, standard error, percentage error and mean precision of measurements of the flat checkerboard and 30-cm tall calibration cube targets by the (a) mono video camera and the (b) stereo camera system (with 600 mm separation between the cameras and in the middle of the images).

| (a)          |             |   |                    |                           |                           |                     |
|--------------|-------------|---|--------------------|---------------------------|---------------------------|---------------------|
| Target       | Measurement | Orientation to lasers                     | Mean error (mm)    | Mean error SE (mm)        | Mean percentage error (%) | Mean Precision (mm) |
| Checkerboard | A           | Horizontal                                | 0.95               | 0.10                      | 0.29                      | 0.80                |
|              | B           | Vertical                                  | 0.46               | 0.06                      | 1.15                      | 0.61                |
|              | C           | Horizontal                                | 0.05               | 0.05                      | 0.25                      | 0.53                |
| Cube         | D           | Diagonal                                  | -3.06              | 0.08                      | -5.38                     | 0.77                |
|              | A           | Both lasers on the cube                   | -0.84              | 0.09                      | -1.25                     | 0.91                |
|              | B           | One laser on cube and one on the seafloor | -6.23              | 0.05                      | -9.04                     | 0.50                |
|              | C           | Both on the seafloor                      | -9.80              | 0.66                      | -24.90                    | 0.69                |
| (b)          |             |   |                    |                           |                           |                     |
| Target       | Measurement | Mean error (mm)                           | Mean error SE (mm) | Mean percentage error (%) | Mean Precision (mm)       |                     |
| Checkerboard | A           | 1.44                                      | 0.06               | 0.45                      | 1.98                      |                     |
|              | B           | 0.13                                      | 0.11               | 0.32                      | 1.11                      |                     |
|              | C           | 0.22                                      | 0.07               | 1.12                      | 0.71                      |                     |
|              | D           | 0.56                                      | 0.05               | 0.97                      | 0.48                      |                     |
| Cube         | A           | -0.65                                     | 0.03               | -0.85                     | 0.31                      |                     |
|              | B           | -0.88                                     | 0.04               | -1.2                      | 0.37                      |                     |
|              | C           | -1.28                                     | 0.03               | -1.79                     | 0.35                      |                     |
|              | D           | -0.09                                     | 0.02               | -0.11                     | 0.22                      |                     |

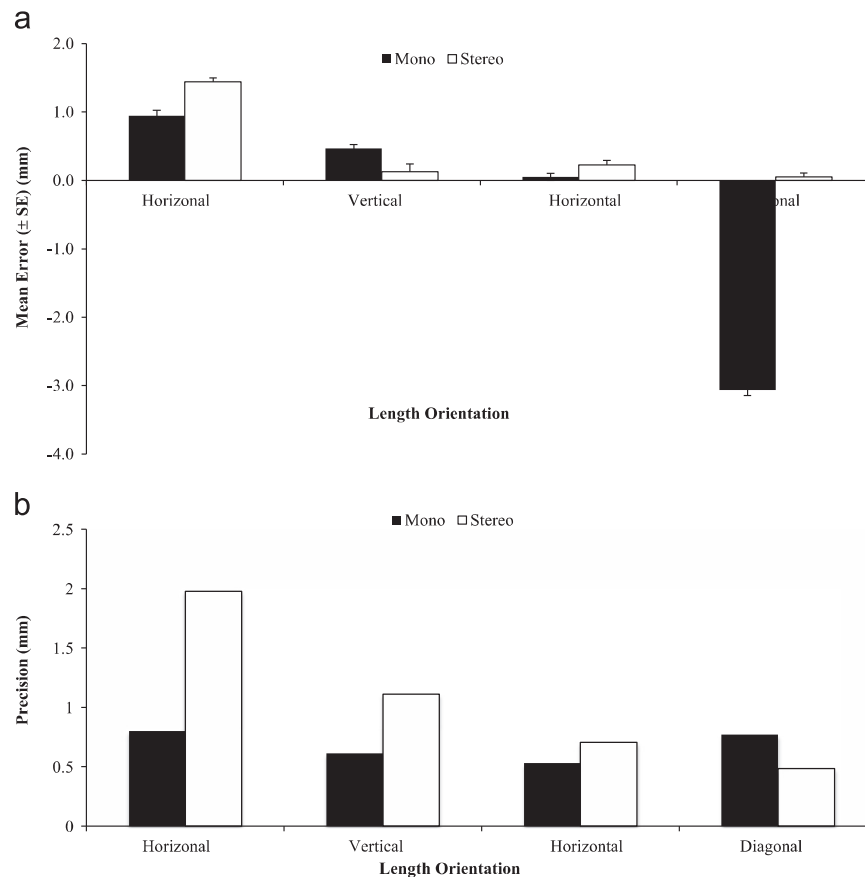


**Fig. 4.** Mean ( $\pm$  SE) measurement (a) error and (b) precision (mm) of length measurement of a flat calibration checkerboard target made by the stereo camera system (open bars) and the mono video camera system (closed bars). Measurements are either made in a horizontal, vertical or diagonal orientation to the paired lasers.

significantly greater ( $V=4$ ,  $N=2069$ ,  $p < 0.05$ ) than that estimated by the mono system (14.58 kg).

For seven species, excluding *O. mutabilis* complex, *P. longicauda* and *P. sp. 2*, significantly greater biomass estimates (all  $p < 0.001$ ) were calculated using data from the stereo system (Fig. 6c). The stereo total biomass estimate in transect two of 12.95 kg was also significantly greater ( $N=1085$ ,  $V=6$ ,  $p < 0.01$ ) than the mono estimate of 7.28 kg (Fig. 7c). The stereo biomass estimates of *E. sp. A*, *P. gracilis*, *P. sp. A*, *P. vitrea* and *S. globosa* were significantly higher (all  $p < 0.001$ ) than VARS estimates.

#### 3.4. Time and cost analysis

The identification and measurement of the 10 megafauna species in a 1 km<sup>2</sup> transect of video footage took approximately 10.5 h, while using the stereo images took approximately 30 h. The total estimated cost of the stereo cameras, housings, strobe equipment and the EventMeasure and CAL software was approximately \$48,000 while the ROV video, housing and lighting system cost approximately \$151,000.

## 4. Discussion

The ability of stereo cameras and measurement software to accurately estimate shallow-water marine fish and invertebrate abundance and size distribution (Abdo et al., 2006; Moore et al., 2010) has led to interest in the application of stereo camera systems in deeper water, but has also raised concerns about calibration of images (Marouchos et al., 2011; Harvey and Shortis, 1998). This study describes initial results from a stereo

camera system and Event Measure software used in the Northeast Pacific abyssal region to estimate the density and length of 10 species of mobile epibenthic megafauna.

#### 4.1. The effect of depth on length measurements

It has been suggested that differences in the refractive index, temperature, salinity and pressure between shallow water where the stereo cameras are calibrated and at depth where surveys are conducted might lead to measurement inaccuracies in stereo measurements (Harvey and Shortis, 1998). Increased water pressure at depth on the camera housings and view ports of a towed stereo-video system resulted in poor measurement accuracy (Shortis et al., 2007). The current study, however, indicated that the shallow-water camera calibration was suitable to achieve accurate and precise measurements during surveys at  $\sim 4000$  m using the configuration described here.

#### 4.2. Stereo camera separation

Separation of the cameras improved measurement accuracy and precision. The disparity, i.e. the difference between the corresponding points of left and right images, is proportional to the baseline separation between the cameras. Therefore, measurements become more accurate and precise as the separation of the cameras increases (Okutomi and Kanade, 1993). The separation cannot be increased indefinitely as overlap of the images must be achieved to enable stereo measurements. However, 600 mm separation provided measurements with an accuracy  $< 1$  mm and a 4 m<sup>2</sup> overlap in image area, which is sufficient for the needs of studies currently conducted as part of the Station M time series.

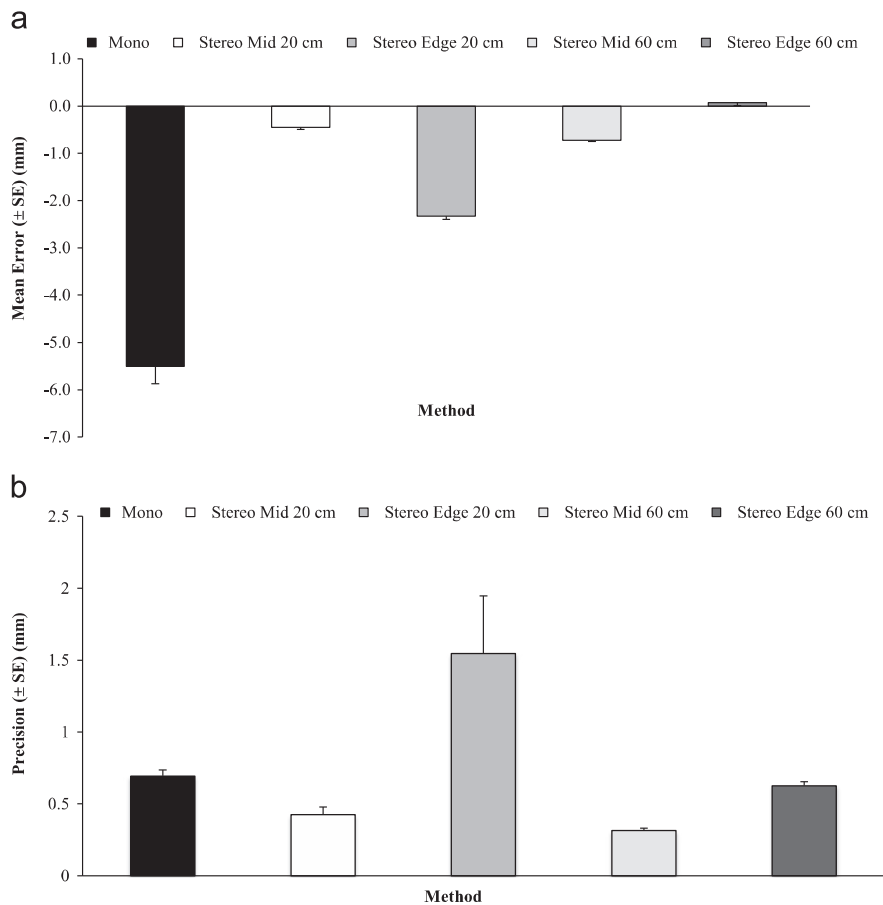


**Fig. 5.** Mean ( $\pm$  SE) measurement of (a) error and (b) precision (mm) of length measurement of a calibration cube target made using the mono video camera system (Mono) and the stereo camera system (Stereo). The stereo cameras were separated by either 200 or 600 mm and measurements were made in the middle (Mid) and edge (Edge) of the images.

#### 4.3. Accuracy and precision of calibration targets measurements

Comparisons between the performance of the stereo cameras and EventMeasure software and a mono video camera and VARS analysis software indicated that both were capable of highly accurate and precise measurements at abyssal depths (approximately  $< \pm 1$  mm measurement error and  $< 1$  mm precision).

The stereo camera measurements of the calibration targets were not restricted by object position or orientation and an accuracy and precision of  $< 1$  mm was achieved for lengths in any orientation where the ends of the object could be clearly recognized. A previous study by Harvey et al. (2002b) compared the accuracy and precision of measurements of plastic fish silhouettes by stereo and mono video camera systems in shallow-water. Harvey et al.'s study also showed that the most accurate and precise length measurements were achieved using a digital stereo video camera system and that stereo measurements were less restricted by target orientation to the camera. A similar result has been obtained in other previous studies of shallow-water stereo camera measurement systems (Harvey and Shortis, 1995; Shortis et al., 2000; Harvey et al., 2010). Klimley and Brown (1983) also concluded that a stereo camera technique was an improvement over single camera systems for measuring the size of free-swimming scalloped hammerhead sharks (*Sphyrna lewini*). Combined with knowledge of size-mass relationships stereo camera systems would be a useful tool to determine the biomass of benthic communities.

The mono video camera used here is mounted at an oblique angle, which causes the spatial scale of the image to consistently change in both the horizontal and vertical planes from the center of the image

in accordance to the Canadian perspective grid (Wakefield and Genin, 1987). The use of lasers to make measurements requires that objects be orientated either horizontally or vertically with respect to the lasers. Relatively low measurement errors ( $< 1$ – $2$  mm) were recorded for calibration target lengths and animals horizontal or vertical to the lasers. However, lengths at a diagonal orientation or not correctly aligned with the lasers were generally underestimated. When the objects measured are in a diagonal orientation relative to the lasers this adds both vertical and horizontal distortion to the measurement causing a significant underestimation (5.38%). This error could be substantially improved by calibrating the field of view based on the Canadian perspective grid.

Paired laser techniques are limited to imaging a target on a flat plane (Barker et al., 2001) and the mono video camera measurement error increased for lengths of the calibration cube that were 30 cm higher than one or both lasers on the seabed. This would lead us to recommend that when measuring objects with VARS, both of the lasers should be on the seabed. Both lasers were on the seabed for the majority of measurements made using VARS in transects one and two. This error could also lead to problems measuring high-relief organisms at Station M, such as sponges on stalks (*Hyalonema* sp), as well as during other benthic transects, when the ROV moves at a constant speed along a heading at a constant altitude above the seabed, taking video of animals of many sizes along the path. During transects the ROV is not able to adjust the view to bring the lasers to the level of organisms that project well above the seafloor. The effect of object height on measurements of the 10 species studied here warrants further investigation, but it is thought that due to their low relief the effect

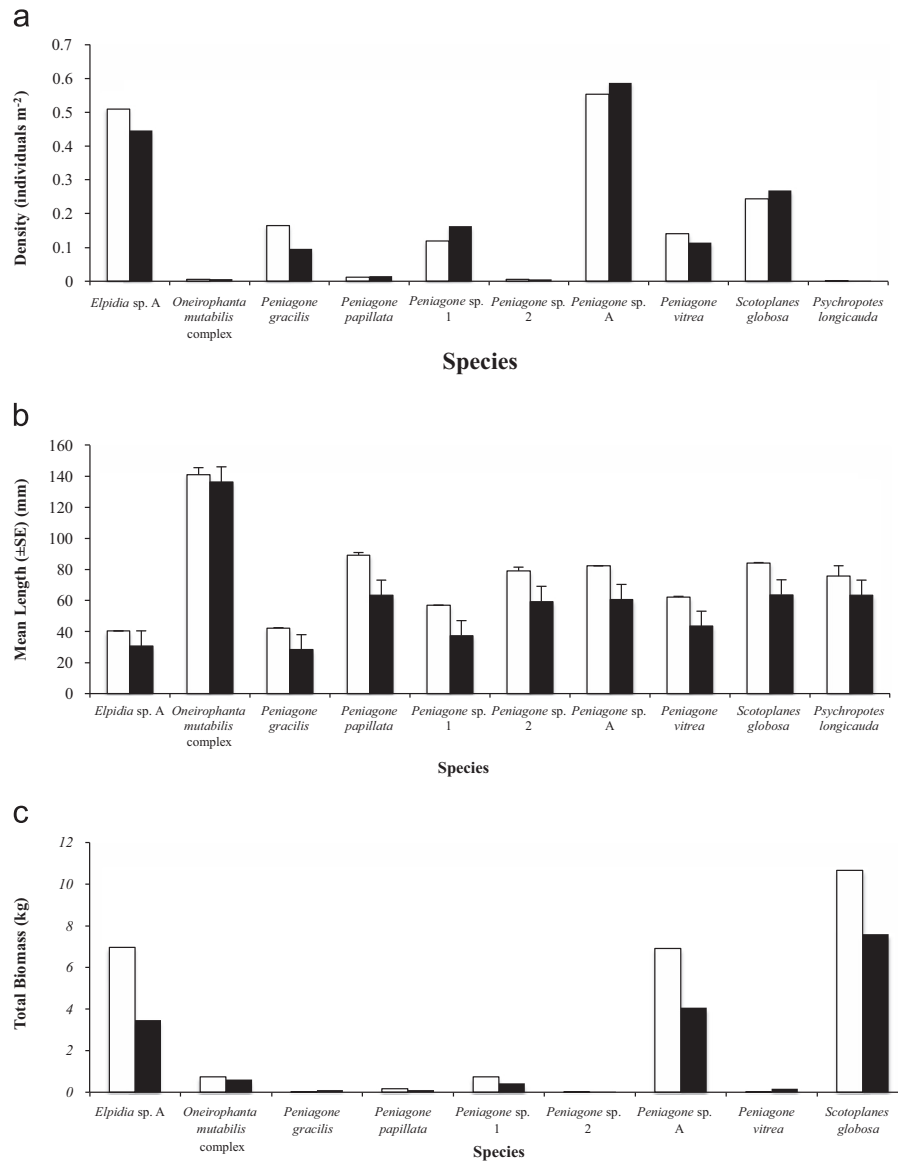


**Fig. 6.** (a) Density (individuals m<sup>-2</sup>), (b) mean length ( $\pm$ SE, mm) and (c) biomass (kg) of 10 megafauna species recorded by the stereo (open bars) and the mono video camera system (closed bars) recorded in Station M transect one.

would be minimal. In contrast, stereo camera measurements appear to be unaffected by the distance of the object to the seabed and would be a useful method to measure high-relief and demersal organisms such as the deep-sea grenadier, *Coryphaenoides armatus*, common at Station M (Priede et al., 1994). Stereo underwater cameras have been used successfully to obtain accurate length measurements of pelagic fish in shallow waters (Santana-Garcon et al., 2014) and this stereo system has the potential to measure deep-sea pelagic organisms.

#### 4.4. Length and biomass estimates of mobile epibenthic megafaunal species

The difference between the stereo and mono megafauna length measurements was amplified when lengths were converted to biomass estimates. Estimates of length and biomass derived from the stereo system were higher than those derived from the mono video camera system for the majority of the 10 megafaunal species studied. The equations describing the length-weight conversion are exponential equations that convert length to a volume, causing errors in the length measurement to be multiplied by the

exponent. This illustrates the importance of accurate and precise length measurements to achieve accurate biomass estimates. The difference between mono and stereo measurements can be partly explained by the error introduced by a proportion of the megafauna in the transects being orientated at a diagonal angle to the lasers. However, the percentage differences in the mean length of megafauna measurements between the methods are generally higher than the mean 5.38% introduced for diagonal length measurements of the checkerboard calibration target (Table 1). Other potential sources of measurement error include the effect of the distance of the organism off the seabed, which has not been quantified for the megafauna. Changes in the tilt of the camera angle due to the movement of the ROV in relation to the seabed may also affect VARS length measurements.

#### 4.5. Time and cost evaluation

It is important to gather large samples of accurate and precise length measurements to detect changes in megafaunal community size structure and biomass over time and in relation to environmental impacts (Abdo et al., 2006). The process of manual selection of length



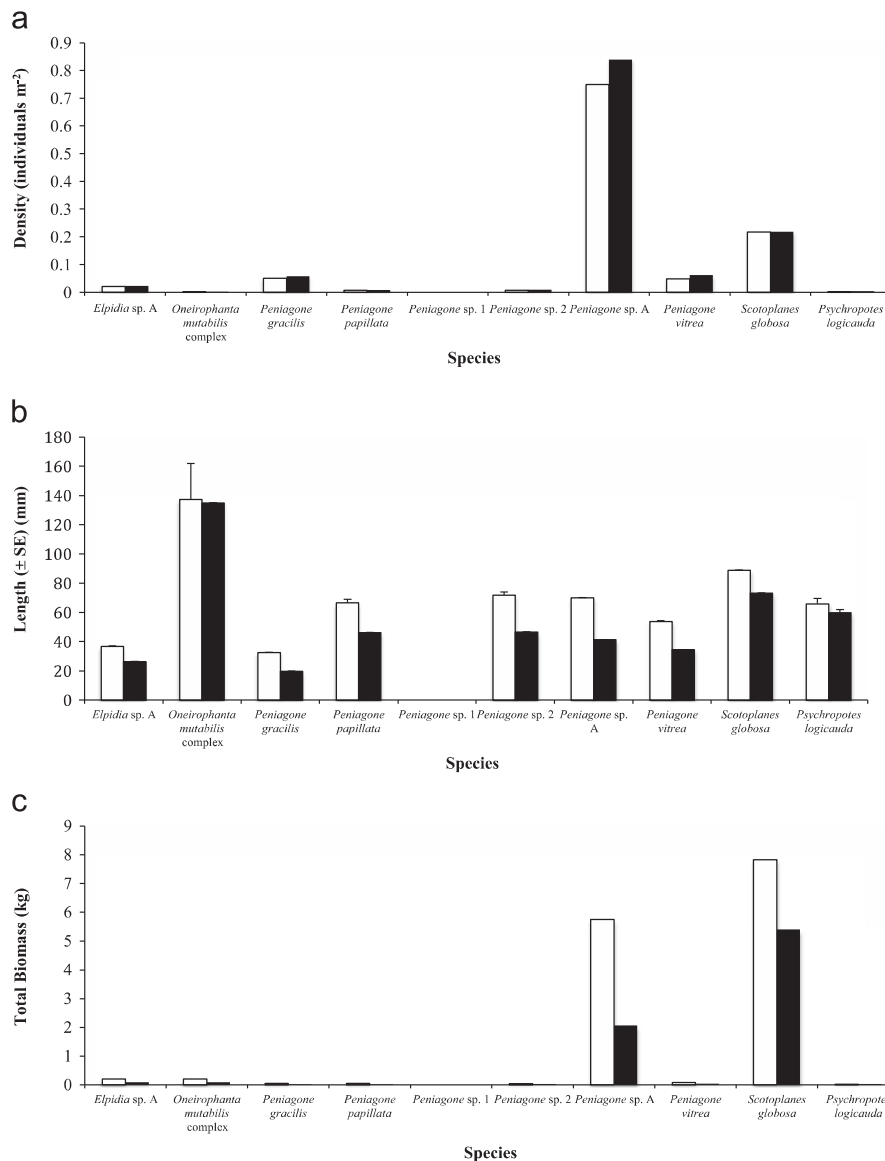


**Fig. 7.** (a) Density (individuals m<sup>-2</sup>), (b) mean length (± SE, mm) and (c) biomass of 10 megafauna species recorded by the stereo (open bars) and the mono video camera system (closed bars) recorded in Station M transect two.

beginning and end points from the stereo images is time consuming (Abdo et al., 2006; Shortis et al., 2013). The automation of species identification and especially measurements should improve the speed of analyzing stereo images (Rosen et al., 2014; Shortis et al., 2013). Studies have reported advances in the automation or semi-automation of the detection, identification and measurement of fish species in underwater camera footage (Shortis et al., 2013). Automation training has found that video sequences are more effective than using a single still image for face recognition algorithms as a series of images can provide more information on the subject in a greater range of orientations (Zhang and Martínez, 2006). The vertical perspective of the stereo system limits the number of orientations of an object that can be captured. The video footage provides a greater range of orientations to the recognition algorithms and advances image analysis automation. However, while the video system enables faster image analysis, the cost of the video equipment is three times that of the stereo camera system. This drawback is offset to some extent by the fact that the video equipment on the ROV can be used for other applications.

The video and stereo still images were analyzed by different observers, which could have introduced an observer bias. The

observer for the video sequences was more experienced in the identification of the 10 megafauna species; however, the density estimates for all species were comparable between the two methods indicating that there was minimal identification error. The stereo technique has previously been found to enable low observer measurement bias (Abdo et al., 2006) but this was not assessed during this study, during which only one observer worked on the stereo measurements. An additional advantage of the stereo system is that it reports an estimation of measurement accuracy automatically using the calibration prior to sampling (Shortis et al., 2007) so that the measurement quality can be assessed throughout the image analysis process.

#### 4.6. Recommendations

Mono video camera measurements require precise placement of the object in a perpendicular orientation to the camera using the ROV to achieve the most accurate measurements. These results suggest that VARS is the most time-effective method to achieve length measurements of these 10 megafauna species; however, the measurement difference associated with individuals not positioned

perpendicularly should be corrected. A correction factor using the Canadian perspective grid system is currently being developed that can be potentially used for VARS, and for other video based measurement techniques using lasers. VARS will thus be able to adjust for the Canadian perspective grid in all stills images, both vertically and horizontally. The stereo camera system measurements are unaffected by object orientation or height therefore making it a potentially suitable technology to be mounted on an autonomous underwater vehicle (AUV) to conduct bottom transects from which estimates of the density, size distribution, and biomass of these 10 megafauna species can be achieved. The use of a long-range AUV to conduct transects at Station M would substantially reduce the logistical commitment and costs involved in producing time-series transects and enable the temporal resolution of sampling at Station M to be increased. The lower unit costs of the stereo camera system in relation to the video camera system may have an advantage for this application, although reductions in the time required to analyse images would be a more effective way to reduce longer-term survey costs.

#### 4.7. Conclusions

Analysis of the density, length and biomass estimates of 10 deep-sea mobile epibenthic megafauna species from the stereo still camera found that the system was capable of high measurement accuracy and precision. The mono video camera system was capable of accurate and precise measurement when objects were perpendicular to the lasers, although the effect of the orientation caused underestimation for calibration target measurements. The effect of the video camera orientation could be compensated with the use of a correction factor. The stereo image analysis process took longer than the video analysis and the value of the Event Measure software tool would be substantially improved with developments in analysis automation. The stereo system is less restricted by object orientation and is potentially a useful tool to be mounted on an AUV to gather length and biomass estimates of mobile deep-sea megafauna.

#### Acknowledgments

This study was supported by the David and Lucile Packard Foundation. We thank John Ferreira for his technical assistance and the crew and ROV pilots of the R/V *Western Flyer* and particularly James Seager for his advice and assistance with the EventMeasure software and stereo camera calibration. We appreciate the constructive comments received from the reviewers.

#### References

- Abdo, D.A., Seager, J.W., Harvey, E.S., McDonald, J.L., Kendrick, G.A., Shortis, M.R., 2006. Efficiently measuring complex sessile epibenthic organisms using a novel photogrammetric technique. *J. Exp. Mar. Biol. Ecol.* 339, 120–133. <http://dx.doi.org/10.1016/j.jembe.2006.07.015>.
- Barker, B.A.J., Davis, D.L., Smith, G.P., 2001. The calibration of laser-referenced underwater cameras for quantitative assessment of marine resources. In: OCEANS, 2001., MTS/IEEE Conference and Exhibition., 3, pp. 1854–1859. <http://dx.doi.org/10.1109/OCEANS.2001.968128>.
- Christiansen, B., Thiel, H., 1992. Deep-sea epibenthic megafauna of the Northeast Atlantic: abundance and biomass at three mid-oceanic locations estimated from photographic transects. In: Rowe, G.T., Pariente, V. (Eds.), *Deep-sea Food Chains and the Global Carbon Cycle*. Academic Publishers, Netherlands, pp. 125–138. <http://dx.doi.org/10.1007/978-94-011-2452-8>.
- Conover, W.J., 1980. *Practical Nonparametric Statistics*. John Wiley, NY.
- Done, T.T., 1982. Photogrammetry in coral ecology: a technique for the study of change in coral communities. In: *Proc. fourth Int. Coral. Reef. Sym.* 2, 315–320.
- Haedrich, R.L., Rowe, G.T., 1977. Megafaunal biomass in the deep sea. *Nature* 269, 141–142. <http://dx.doi.org/10.1038/269141a0>.
- Harvey, E.S., Goetze, J., McLaren, B., Langlois, T., Shortis, M.R., 2010. Influence of range, angle of view, image resolution and image compression on underwater stereo-video measurements: high-definition and broadcast-resolution video cameras compared. *Mar. Technol. Soc. J.* 44, 75–85. <http://dx.doi.org/10.4031/MTSJ.44.1.3>.
- Harvey, E., Shortis, M., 1995. A system for stereo-video measurement of sub-tidal organisms. *Mar. Technol. Soc. J.* 29, 10–22.
- Harvey, E.S., Shortis, M.R., 1998. Calibration stability of an underwater stereo-video system: implications for measurement accuracy and precision. *Mar. Technol. Soc. J.* 32, 3–17.
- Harvey, E., Fletcher, D., Shortis, M., 2002a. Estimation of reef fish length by divers and by stereo-video: a first comparison of the accuracy and precision in the field on living fish under operational conditions. *Fish. Res.* 57, 255–265. [http://dx.doi.org/10.1016/S0165-7836\(01\)00356-3](http://dx.doi.org/10.1016/S0165-7836(01)00356-3).
- Harvey, E., Shortis, M., Stadler, M., Cappo, M., 2002b. A comparison of the accuracy and precision of measurements from single and stereo-video systems. *Mar. Technol. Soc. J.* 36, 38–49. <http://dx.doi.org/10.4031/002533202787914106>.
- Harvey, E.S., Newman, S.J., McLean, D.L., Cappo, M., Meeuwig, J.J., Skepper, C.L., 2012. Comparison of the relative efficiencies of stereo-BRUVs and traps for sampling tropical continental shelf demersal fishes. *Fish. Res.* 125, 108–120. <http://dx.doi.org/10.1016/j.fishres.2012.01.026>.
- Grassle, J.F., Sanders, H.L., Hessler, R.R., Rowe, G.T., McLellan, T., 1975. Pattern and zonation: a study of the bathyal megafauna using the research submersible *Alvin*. *Deep Sea Res.* 22, 457–481. [http://dx.doi.org/10.1016/0011-7471\(75\)90020-0](http://dx.doi.org/10.1016/0011-7471(75)90020-0).
- Janßen, F., Treude, T., Witte, U., 2000. Scavenger assemblages under differing trophic conditions: a case study in the deep Arabian Sea. *Deep Sea Res.* 47, 2999–3026. [http://dx.doi.org/10.1016/S0967-0645\(00\)00056-4](http://dx.doi.org/10.1016/S0967-0645(00)00056-4).
- Kaufmann, R.S., Smith Jr, K.L., 1997. Activity patterns of mobile epibenthic megafauna at an abyssal site in the eastern North Pacific: results from a 17-month time-lapse photographic study. *Deep Sea Res.* 44, 559–579. [http://dx.doi.org/10.1016/S0967-0637\(97\)00005-8](http://dx.doi.org/10.1016/S0967-0637(97)00005-8).
- Klimley, A.P., Brown, S.T., 1983. Stereophotography for the field biologist: measurement of lengths and three-dimensional positions of free-swimming sharks. *Mar. Biol.* 74, 175–185. <http://dx.doi.org/10.1007/BF00413921>.
- Kuhnz, L.A., Ruhl, H.A., Huffard, C.A., Smith, K.L., 2014. Rapid changes and long-term cycles in the benthic megafaunal community observed over 24 years in the abyssal northeast Pacific. *Prog. Oceanogr.* 124, 1–11. <http://dx.doi.org/10.1016/j.pocean.2014.04.007>.
- Lampitt, R.S., Billett, D.S.M., Rice, A.L., 1986. Biomass of the invertebrate megabenthos from 500 to 4100 m in the northeast Atlantic Ocean. *Mar. Biol.* 93, 69–81. <http://dx.doi.org/10.1007/BF00428656>.
- Langlois, T.J., Fitzpatrick, B.R., Fairclough, D.V., Wakefield, C.B., Hesp, S.A., McLean, D.L., Harvey, E.S., Meeuwig, J.J., 2012. Similarities between line fishing and baited stereo-video estimations of length-frequency: novel application of kernel density estimates. *PLoS One* 7, e45973. <http://dx.doi.org/10.1371/journal.pone.0045973>.
- Lauerman, L.M.L., Kaufmann, R.S., 1998. Deep-sea epibenthic echinoderms and a temporally varying food supply: results from a one year time series in the NE Pacific. *Deep Sea Res.* 45, 817–842. [http://dx.doi.org/10.1016/S0967-0645\(98\)00004-6](http://dx.doi.org/10.1016/S0967-0645(98)00004-6).
- Lauerman, L.M.L., Kaufmann, R.S., Smith Jr, K.L., 1996. Distribution and abundance of epibenthic megafauna at a long time-series station in the abyssal northeast Pacific. *Deep Sea Res.* 43, 1075–1103. [http://dx.doi.org/10.1016/0967-0637\(96\)00045-3](http://dx.doi.org/10.1016/0967-0637(96)00045-3).
- Marouchos, A., Sherlock, M., Barker, B., Williams, A., 2011. Development of a stereo deepwater baited remote underwater video system (DeepBRUVs). In: OCEANS, 2011., MTS/IEEE Conference and Exhibition., pp. 1–5. <http://dx.doi.org/10.1109/Oceans-Spain.2011.6003410>.
- Moore, C.H., Harvey, E.S., Van Niel, K., 2010. The application of predicted habitat models to investigate the spatial ecology of demersal fish assemblages. *Mar. Biol.* 157, 2717–2729. <http://dx.doi.org/10.1007/s00227-010-1531-4>.
- Okutomi, M., Kanade, T., 1993. A multiple-baseline stereo. *IEEE Trans. Pattern Anal.* 15, 353–363. <http://dx.doi.org/10.1109/34.206955>.
- Pelaez, J., McGowan, J.A., 1986. Phytoplankton pigment patterns in the California Current as determined by satellite. *Limnol. Oceanogr.* 31, 927–950.
- Priede, I.G., Bagley, P.M., Smith Jr, K.L., 1994. Seasonal change in activity of abyssal demersal scavenging grenadiers *Coryphaenoides (Nematonurus) armatus* in the eastern North Pacific Ocean. *Limnol. Oceanogr.* 39, 279–285. [http://dx.doi.org/10.1016/0198-0149\(90\)90030-Y](http://dx.doi.org/10.1016/0198-0149(90)90030-Y).
- R Development Core Team, 2011. *R: A Language and Environment for Statistical Computing*. R Foundation for Statistical Computing, Vienna, Austria.
- Rochet, M.J., Cadiou, J.F., Trenkel, V.M., 2006. Precision and accuracy of fish length measurements obtained with two visual underwater methods. *Fish. Bull. Nat. Oceanic Atmos.* 104, 1–9.
- Rosen, S., Jørgensen, T., Hammersland-White, D., Holst, J.C., 2014. DeepVision: a stereo camera system provides highly accurate counts and lengths of fish passing inside a trawl. *Can. J. Fish. Aquat. Sci.* 70, 1456–1467. <http://dx.doi.org/10.1139/cjfas-2013-0124>.
- Ruhl, H.A., 2007. Abundance and size distribution dynamics of abyssal epibenthic megafauna in the northeast Pacific. *Ecology* 88, 1250–1262. <http://dx.doi.org/10.1890/06-0890>.
- Ruhl, H.A., 2008. Community change in the variable resource habitat of the abyssal northeast Pacific. *Ecology* 89, 991–1000. <http://dx.doi.org/10.1890/06-2025.1>.
- Ruhl, H.A., Smith Jr, K.L., 2004. Shifts in deep-sea community structure linked to climate and food supply. *Science* 305, 513–515. <http://dx.doi.org/10.1126/science.1099759>.
- Ruhl, H.A., Bett, B.J., Hughes, S.J.M., Alt, C.J.S., Ross, E.J., Lampitt, R.S., Pebody, C.A., Smith Jr, K.L., Billett, S.M., 2013. Links between deep-sea respiration and

- community dynamics. *Ecology* 95, 1651–1662. <http://dx.doi.org/10.1890/13-0675.1>.
- Santana-Garcon, J., Newman, S.J., Harvey, E.S., 2014. Development and validation of a mid-water baited stereo-video technique for investigating pelagic fish assemblages. *J. Exp. Mar. Biol. Ecol.* 452, 82–90. <http://dx.doi.org/10.1016/j.jembe.2013.12.009>.
- Schlining, B.M., Stout, N.J., 2006. MBARI's video annotation and reference system. In: OCEANS, 2006., MTS/IEEE Conference and Exhibition., pp. 1–5. <http://dx.doi.org/10.1109/OCEANS.2006.306879>.
- Shortis, M.R., Miller, S., Harvey, E.S., Robson, S., 2000. An analysis of the calibration stability and measurement accuracy of an underwater stereo-video system used for shellfish surveys. *Geomatics Res. Australas.* 1–24.
- Shortis, M.R., Harvey, E.S., 1998. Design and calibration of an underwater stereo-video system for the monitoring of marine fauna populations. *Int. Arch. Photogramm. Remote Sens.* 32, 792–799.
- Shortis, M.R., Seager, J.W., Williams, A., Barker, B.A., Sherlock, M., 2007. A towed body stereo-video system for deep water benthic habitat surveys. In: Eighth Conference on Optical 3D, Swiss Federal Institute of Technology. Zurich. pp. 150–157.
- Shortis, M.R., Ravanbaksh, M., Shaifat, F., Harvey, E.S., Mian, A., Seager, J.W., Culverhouse, P.F., Cline, D.E., Edgington, D.R., 2013. A review of techniques for the identification and measurement of fish in underwater stereo-video image sequences. In: SPIE Optical Metrology 2013., International Society for Optics and Photonics., pp. 87910–87910.
- Smith Jr, K.L., Kaufmann, R.S., Edelman, J.L., Baldwin, R.J., 1992. Abyssopelagic fauna in the central North Pacific: comparison of acoustic detection and trawl and baited trap collections to 5800 m. *Deep Sea Res* 39, 659–685. [http://dx.doi.org/10.1016/0198-0149\(92\)90094-A](http://dx.doi.org/10.1016/0198-0149(92)90094-A).
- Smith Jr, K.L., Kaufmann, R.S., Wakefield, W.W., 1993. Mobile megafaunal activity monitored with a time-lapse camera in the abyssal North Pacific. *Deep Sea Res* 40, 2307–2324. [http://dx.doi.org/10.1016/0967-0637\(93\)90106-D](http://dx.doi.org/10.1016/0967-0637(93)90106-D).
- Smith Jr, K.L., Ruhl, H.A., Kahru, M., Huffard, C.L., Sherman, A.D., 2013. Deep ocean communities impacted by changing climate over 24 y in the abyssal northeast Pacific Ocean. *Proc. Natl. Acad. Sci. U.S.A.* 110, 19838–19841. <http://dx.doi.org/10.1073/pnas.1315447110>.
- Smith Jr, K.L., Sherman, A.D., Huffard, C.L., McGill, P.R., Henthorn, R., Von Thun, S., Ruhl, H.A., Kahru, M., Ohman, M.D., 2014. Large salp bloom export from the upper ocean and benthic community response in the abyssal northeast Pacific: day to week resolution. *Limnol. Oceanogr.* 59, 745–757. <http://dx.doi.org/10.4319/lo.2014.59.3.0745>.
- Wakefield, W.W., Genin, A., 1987. The use of a Canadian (perspective) grid in deep-sea photography. *Deep Sea Res* 34, 469–478. [http://dx.doi.org/10.1016/0198-0149\(87\)90148-8](http://dx.doi.org/10.1016/0198-0149(87)90148-8).
- Zhang, Y., Martínez, A.M., 2006. A weighted probabilistic approach to face recognition from multiple images and video sequences. *Image Vision Comput.* 24, 626–638. <http://dx.doi.org/10.1016/j.imavis.2005.08.004>.